Proceedings of the 2012 International Conference on Industrial Engineering and Operations Management
Istanbul, Turkey, July 3 – 6, 2012

Virtual Optimization of a Wireless, Solar PV/Wind Hybrid System Controller for Street-Lighting Applications based on Environmental Conditions in Greater Toronto Area

S.E. Sadique
School of Mechanical Engineering, Sheridan College
7899 McLaughlin Road, Brampton, ON
L6Y 5H9, Canada

Ahad Ali
A. Leon Linton Dept. of Mechanical Engineering
Lawrence Technological University, 21000 West Ten Mile Road
Michigan 48075, USA

D. Wang
Department of Advanced Manufacturing and Automation Technology
Centennial College, 941 Progress Avenue, Toronto, ON
M1G3T8 Canada

Abstract

In this study, HOMER software has been used to perform simulations of hybrid (solar PV/wind) systems for street-lighting applications. HOMER allows the designer to compare many different design options based on their technical and economic merits. Statistical analysis of the collected high resolution (10 minutes) data for CEI and monthly averaged Environment Canada data of Toronto Int'l Airport (TIA) was also performed. In all, 32 different hybrid PV/wind system scenarios were simulated to estimate the cost and determine the feasibility of a system design using CEI and TIA datasets. Moreover, system sensitivity analyses were performed using sensitivity variables such as wind turbine hub height and annual capacity shortage. In summary, the 10-min solar/wind resolution data has an impact on the hybrid solar/wind system design. As a result of the analysis of simulation results the following recommendations may be made: (i) It is necessary to compare the computer simulations to long term performance measurements of an actual operating hybrid PV/wind system for street lighting, to corroborate the simulation results. (ii) Since only two well-known micro-wind turbines were studied, it would be beneficial to study other emerging micro wind turbine options with higher performance in the 1-4 m/s range and simulate their performance using HOMER software, as well as in physical testing. This is in order to determine if such technologies are able to provide distinct advantages over solar-only configurations.

Keywords
HOMER, Hybrid street-lighting Statistical analysis, Simulations.

1. Introduction
Territories and rural areas in Canada is a geographically isolated from mainland. Electrical power needs are supplied by a large number of local power companies. Due to the isolation of many dwellings, agricultural sites, and industrial sites, there is considerable interest in novel forms of electricity production. Two such forms of production are solar photo-voltaic (PV) cells based on DC power generating arrays and wind turbines based on propeller-driven DC power generators. Electrical power generation and special sources of electric power, like wind-turbines, are frequently discussed in the public media. The additional factor of the general concern and interest for environmental issues is a further enticement to attract the student's interest in these "green-technology" forms of electricity generation.

Distributed electricity generation from Renewable Energy Sources (RES) such as solar and wind are increasingly seen as cost effective alternatives to centralized carbon-based generation. A disadvantage, common to wind and solar options, however, is their unpredictable nature and dependence on weather and climatic changes. The hybrid systems that combine solar and wind generating units with battery backup can attenuate their individual fluctuations and reduce energy storage requirements significantly. However, some problems stem from the increased complexity of the system in comparison with single energy systems. This complexity, brought about by the use of two different resources combined, makes an analysis of hybrid systems more difficult (Yang et al., 2008). In order to efficiently and economically utilize the renewable energy resources, an optimum match design sizing method is necessary. Various optimization techniques such as the probabilistic approach, graphical construction method, iterative and artificial intelligence (AI) techniques have been recommended by researchers.

Tina et al. (2006) presented a probabilistic approach based on the convolution technique to incorporate the fluctuating nature of the resources and the load, thus eliminating the need for time-series data, to assess the long-term performance of a hybrid solar–wind system for both stand-alone and grid-connected applications. A graphical construction technique for figuring the optimum combination of battery and PV array in a hybrid solar–wind system has been presented by Borowy and Salameh (1996). Yang et al. (2003, 2007) have proposed an iterative optimization technique following the loss of power supply probability (LPSP) model for a hybrid solar-wind system. The number selection of the PV module, wind turbine and battery ensures the load demand according to the power reliability requirement, and the system cost is minimized. Similarly, an iterative optimization method was presented by Kellogg et al. (1998) to select the wind turbine size and PV module number needed to make the difference of generated and demanded power (DP) as close to zero as possible over a period of time.

Ekren and Ekren (2009) conducted the optimization of a hybrid PV/wind system using a simulation based optimization procedure, OptQuest, which integrates various heuristic methods. Ekren and Ekren (2008) used the response surface methodology (RSM) in size optimization of an autonomous PV/wind integrated hybrid energy system with battery storage. RSM is a collection of statistical and mathematical methods which relies on optimization of response surface with design parameters. Diaf et al. (2007) presented a methodology to perform the optimal sizing of an autonomous hybrid PV/wind system according to the loss of power supply probability (LPSP) and the levelized cost of energy (LCE) concepts. The methodology aims at finding the configuration, among a set of systems components, which meets the desired system reliability requirements, with the lowest value of levelized cost of energy. Eftichios Koutroulis et al. (2006) developed a methodology for optimal sizing of stand-alone PV/wind-generator systems. The proposed methodology is based on the genetic algorithms (GA) and compared with linear programming. Yang et al. (2008) developed an optimal sizing model for a stand-alone hybrid solar–wind system employing battery banks based on the loss of power supply probability (LPSP) and the annualized cost of system (ACS) concepts. Taskin et al. (2009) presented an evaluation of the combined solar and wind system for highway energy requirements such as lighting, SOS, billboard etc. A new model Savonius wind turbine was designed and its prototype was manufactured.

Currently various software (models) have been developed for simulation Renewable Energy (REN) systems. Examples include HOMER, Hybrid2, INSEL, MATLAB, PROLOAD, RETScreen, RPM-Sim, SIMENERG, WDLTOOLS, WINSYS. In this study, the response surface, output performance measure, is the hybrid system cost, and the design parameters are the PV size, wind turbine rotor swept area and the battery capacity. HOMER (Hybrid Optimization Model for Electrical Renewables) software was used to perform simulation of a hybrid PV/wind system for street-lighting applications using performance characteristics of Global Power Design's (GPD) controller, selected solar and wind generators, as well as Centennial College's 5-year, high resolution 10 minutes solar and wind dataset. HOMER allows the designer to compare many different design options based on their technical and economic merits.

Key Objectives of this project are:

a) Determine the effect of solar/wind data resolution on the system design and its value for future end user and commercial point of power applications
b) Determine which system would require the least energy storage and lowest projected system capital cost.
c) Set expectations for a physical installation and testing of controller prototypes in a phase II "proof of product" research project, to be completed under the FedDev Applied Research & Commercialization Initiative.

2. Equipment and Methodology

The hybrid PV/Wind system for street lighting includes the following components (Figure 1) photovoltaic (PV) panels, 2) wind turbine, 3) batteries, 4) controller and 5) street lamp (load). Power generated by the PV array during the day is stored in the battery bank through the energy controller, which controls the complete system. The wind generator starts generating power when wind reaches the cut-in speed and the output is stored also in the battery bank. The stored energy is drawn by the electrical load (street lamp) through the controller. The battery bank is designed to feed the loads up to a certain number of days with no sun or wind, depending upon the system requirement.

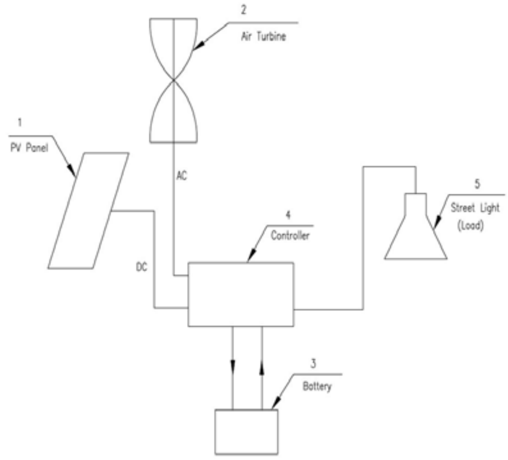

Figure 1: Hybrid PV-Wind System Street Lighting Schematic Diagram.

2.1 Location

All scenarios have been simulated for Toronto, Ontario climate conditions using CEI and TIA dataset resources:

- Latitude = 43°40′
- Longitude = 79°24′

Toronto's continental climate is moderated by Lake Ontario; its climate is among the mildest in Canada east of the Rocky Mountains. It sits in a pocket of the humid continental climate zone found at the south-western end of Lake Ontario covering the southern part of the city - including downtown, where the annual average temperature exceeds 9 °C (48 °F). There is a high degree of variability from year to year and sometimes even over a period of days, particularly during the winter months (Environne- ment Canada, since 1871). The summary of the hybrid PV/ wind system's components used in this study is shown in Table 1.

Table 1: Hybrid PV/ Wind System Components

No.	COMPONENT	CAPACITY	COST	DETAILS
1	1.1 Solar PV module 1.2 Solar PV module	175 Wp 215 Wp	$3 per Watt	*SunTech mono-crystalline Si*, Efficiency = 13.67% Temperature coeff. of power = -0.47 % / ^{o}C Nominal cell operating temperature = 45 ^{o}C *Sanyo mono-crystalline Si*, Module Efficiency: 17.1% Cell Efficiency: 19.3%
2	2.1 Wind Turbine 2.2 Wind Turbine	70 W, 10 m/s 146 W, 10 m/s	$1,200 per unit $1,000 per unit	GUS-1B by Greenpower Utility Systems AIR-X by Southwest Windpower
3	Battery	105 Ah, 12V	$250 per unit	FullRiver
4	Streetlight 4.1 LED 4.2 LED	35 W 57 W ON all night	$600	King Luminaire
5	5.1 Pole 5.2 Arm 5.3 Battery compartment 5.4 Transport & hole 5.5 Installation, 4h at $75		$1,500 $500 $1,000 $500 $300	Efston Science

3. Climate Data and Load

Two sets of environmental recourses data have been used to simulate the Hybrid PV/Wind system's scenarios: (i) Centennial College's solar/wind 5-year data set, with high 10-minute resolution and (ii) Toronto Int'l Airport's (TIA) monthly average data.

3.1 Centennial Energy Institute (CEI) Data

The Environmental Data Collection tower used at Centennial College's meteorological station is the 30-meter (100') NRG NOW System-Symphonie.

3.1.1 Solar Insolation Data

The baseline data is a one-year time series representing the average global solar radiation on the horizontal surface, expressed in kWh/m^2, for each time step of the year. HOMER displays the monthly average radiation and clearness index of the baseline data in the solar resource table and graph. There are two ways to create baseline data: HOMER is used to synthesize hourly data from monthly averages, or time series radiation data are imported from a file. To synthesize data, the user must enter twelve average monthly values of either solar radiation or clearness index. As the user enters values in the table, HOMER builds a set of 8,760 solar radiation values, or one for each hour of the year. HOMER creates the synthesized values using the Graham algorithm, which results in a data sequence that has realistic day-to-day and hour-to-hour variability and autocorrelation. HOMER detects the time step when the user imports the data file. For example, if the data file contains 8760 lines, HOMER will assume that it contains hourly data. If the data file contains 52,560 lines, HOMER will assume that it contains 10-minute data (National Renewable Energy Laboratory, 2005 and Lambert et al., 2006). The text file that contains the Centennial College's 10-minute solar radiation data has been prepared and used for simulation in this study. Also, solar radiation monthly averages were determined for each year and four years respectively using CEI resource data.

Figure 2 shows the global horizontal solar radiation monthly averages (kWh/m^2/day) variation for four years: 2006, 2007, 2008 and 2009. As can be seen (Figure 2), although the solar radiation monthly averages data vary from year to year, the annual averages data are almost the same for four years.

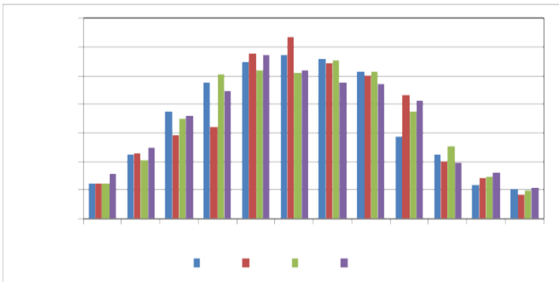

Figure 2: Global Horizontal Solar Radiation Monthly Averages (kWh/m^2/day) Variation

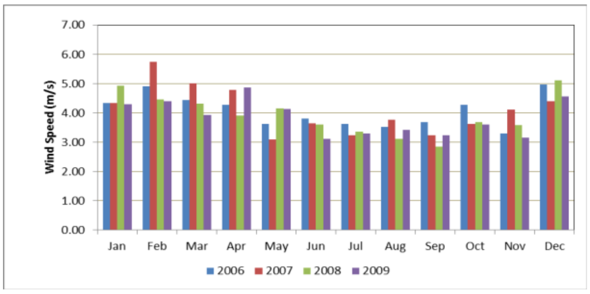

Figure 3: Wind Speed Monthly Averages (m/s) Variation

3.1.2 Wind Speed Data

The text file that contains the Centennial College's 10-minute wind speed data has been prepared and used for simulation in this study. Also, wind speed monthly averages were determined for each year and four years respectively using CEI resource data. Figure 3 shows the wind speed monthly averages (m/s) variation for four years: 2006, 2007, 2008 and 2009. As can be seen (Figure 3) the wind speed monthly averages data vary from month to month and from year to year, but the annual averages data are almost the same for four years.

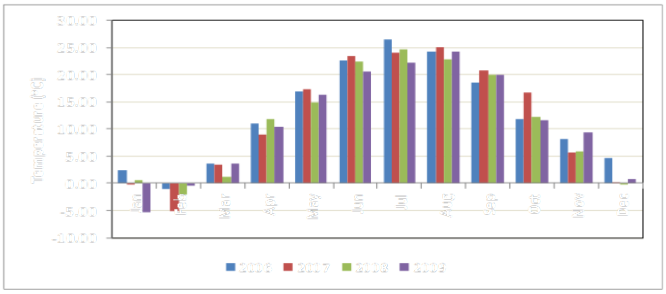

Figure 4: Air Temperature Monthly Averages (**^{o}C)** Variation

3.1.3 Air Temperature Data

The text file that contains the Centennial College's 10-minute air temperature data has been prepared and used for simulation in this study. Also, air temperature monthly averages were determined for each year and four years respectively using CEI resource data. Figure 4 shows the air temperature monthly averages (^{o}C) variation for four years: 2006, 2007, 2008 and 2009.

3.2 Toronto Int'l Airport (NASA) Data

Environment Canada's weather service – the Meteorological Service of Canada (MSC) has been collecting environmental data and translating these into practical weather prediction tools and services since 1871 (Environne- ment Canada, since 1871). The MSC maintains weather collecting stations throughout Canada's territories, one of which is located at Pearson International Airport located in the western environs of the GTA. In the case of long-term weather data for solar insolation, wind data air temperature, etc. the MSC has published monthly averages. These averages, however, are based on data collected over the period from 1971 to 2000. This is about to be updated in 2011.

3.2.1 Solar Insolation Data

Solar radiation is the measurement of radiant energy from the sun, on a horizontal surface. There are several standardized components of independent measurements. Each component is assigned a different identifying number referred to as Radiation Fields (RF). The standard metric unit of radiation measurement is the Mega Joule per square meter (MJ/m^2) (Climate Weather Office). The TIA's global horizontal solar radiation monthly averages data are available in RETScreen resource data (RETScreen, 2005). Components measured and used by MSC:

i. RF1: Global Solar Radiation: the total incoming direct and diffuse short-wave solar radiation received from the whole dome of the sky on a horizontal surface.
ii. RF2: Sky Radiation (Diffuse): the portion of the total incoming short-wave solar radiation received on a horizontal surface that is shielded from the direct rays of the sun by means of a shade ring.
iii. RF3: Reflected Solar Radiation: the portion of the total incoming short-wave radiation that has been reflected from the Earth's surface and diffused by the atmospheric layer between the ground and the point of observation onto a horizontal surface.
iv. RF4: Net Radiation: the resultant of downward and upward total (solar, terrestrial surface, and atmospheric) radiation received on a horizontal surface (RF1 + RF2 + RF3).

3.2.2 Wind Speed Data

Most principal climatological stations are equipped with a standard type U2A anemometer, taking one-minute or (since 1985 two-minute mean speeds values at each observation. At other wind-measuring sites, values are usually obtained from autographic records of U2A or 45B anemometers. Averaging periods at these sites may vary from one minute to an hour (Climate Weather Office). In observing, wind speed is measured in nautical miles per hour and converted to kilometers per hour. The extreme gust speed is the instantaneous peak wind observed from the anemometer dials, or abstracted from a continuous chart recording. A value of zero (0) denotes a calm or no wind.

Wind directions measured by U2A's are recorded to the nearest ten degrees, while those from the 45B are provided to 8 points of the compass. All wind directions are defined as the direction from which the wind blows with respect to true or geographic north. For example, an easterly wind is blowing from the east, not toward the east. A wind direction observation represents the average direction over the two minutes period ending at the time of observation. The most frequent wind direction is based on the number of occurrences of each of the 36 possible directions for each month. A monthly average is calculated for each direction for all months having sufficient record (90% complete for hourly elements). The direction with the highest average count is assigned as the most frequent wind direction for the month. The most frequent wind direction for the year is simply deduced as the direction with the highest average occurrence count for all months.

Wind speed and direction are greatly affected by proximity to the ground and by the presences of obstacles such as hills, buildings and trees. It tends to increase in speed and veer with height above ground. For meteorological purposes, the standard exposure of anemometer cups is at a height of 10 metres above the ground surface. The TIA's wind speed monthly averages data are available in RETScreen resource data (RETScreen, 2005).

3.2.3 Air Temperature Data

Temperature measurements are made from self-registering maximum and minimum thermometers set in a louvered, wooden shelter. The shelter is mounted on a stand so that the thermometers are approximately 1.5 m above ground, which is usually a level, grassy surface. At most climatological stations, maximum temperature is the highest temperature recorded in a 24-hour period ending in the morning of the next day. The minimum values are for a period of the same length, beginning in the evening of the previous day. Mean temperature is the average of the two. At most principal stations, the climatological day begins at 0600 UTC (Universal Time Coordinate) and ends at the onset of 0600 UTC on the following day. These times are equivalent or close to midnight local standard time for most of Canada (Climate Weather Office). The TIA's air temperature monthly averages data are available in RETScreen resource data (RETScreen, 2005).

3.3 The Difference between CEI's and Toronto Int'l Airport's Environmental Data

Current estimates of environmental data showed (revealed) that climate data from various sources vary sometimes widely. Effects of micro-climates are not well known. Reliable data sources are often interpolated over large distances, or supplemented by satellite-derived data which still suffer from serious shortcomings. More work is needed to increase the reliability and spatial coverage of solar radiation estimates (Thevenard et al., 2010).

3.3.1 Solar Insolation Data

The CEI's and TIA's global horizontal solar radiation monthly averages data are compared. Figure 5 shows the comparison between CEI's and TIA's global horizontal solar radiation monthly averages (kWh/m^2/day) variation.

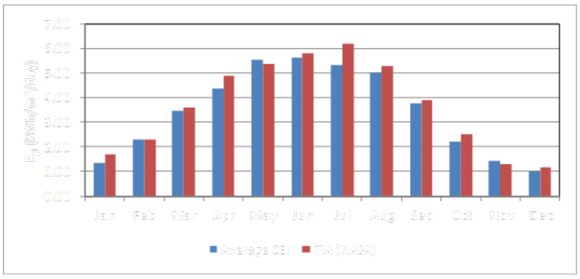

Figure 5: Global Horizontal Solar Radiation Monthly Averages (kWh/m^2/day) Variation

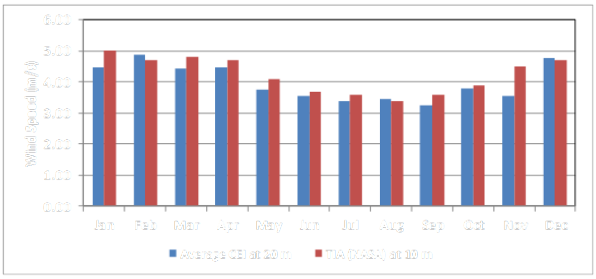

Figure 6: Wind Speed Monthly Averages (m/s) Variation

3.3.2 Wind Speed Data

The CEI's and TIA's wind speed monthly averages data are compared. Figure 6 shows the comparison between CEI's and TIA's wind speed monthly averages (m/s) variation. The analysis of wind speed distribution histograms (Figure 6) shows that within a range of 2.0 to 5.0 m/s the wind speed frequency has the maximum values and varies from 200 to 450.

3.3.3 Air Temperature Data

The CEI's and TIA's air temperature monthly averages data are plotted in Figure 7. It shows the comparison between CEI's and TIA's air temperature monthly averages (^oC) variation. As can be seen from Figures 5, 6 and 7 the climate data from CEI and TIA sources vary from month to month since the CEI's data are monthly average for four years while TIA's data are average for a 30 years period.

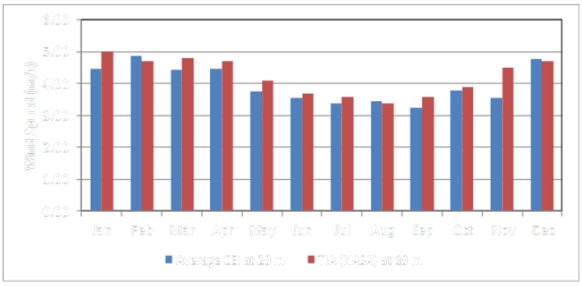

Figure 7: Air Temperature Monthly Averages (**^{o}C)** Variation

5. Load

Two types of LED lights of 57 W and 35 W each are used. The street lights are switched on when the intensity of solar radiation is zero in the evening and they are switched off at first light when the intensity of solar radiation is greater than zero. Time Series Data (10 minutes averages) has been used. In one Scenario the load profile incorporates dimming of the street lights from midnight 00:00 - 04:00 AM when the wattage of light is reduced to 67%. The 57W light is dimmed to 39W (Figure 8). A more realistic, complex load profile will consider Dusk to Dawn operation of the street lights and take into account variation in daylight hours. This will be based on the actual times of Sunrise and Sunset, and can be inputted as an Hourly Time Series Load Profile. A High Efficiency LED Light Fixture is claimed to throw the same amount of light on the street as sodium vapor lights at 1/10th the power consumption with only a slight lumen depreciation after 70,000 hours.

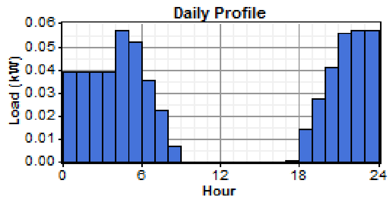

(a)

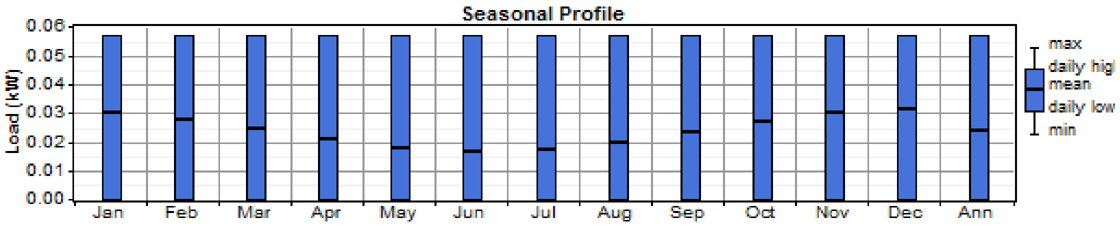

(b)

Figure 8: 57 W Load (with dimming) Profile: (a) Daily and (b) Seasonal

6. Hybrid Pv/Wind System For Street Lighting Simulation Scenarios

For all Scenarios: The climate data used for the different Scenarios remain the same. This includes temperature, solar and wind resource data. Moreover, all Scenarios use one of the two basic Load Profiles.

Assumptions:

- Location - GTA, Toronto
- Project Lifetime - 20 years
- System fixed O&M cost - Zero $
- System voltage - 24 V
- Battery - 105 AH, 12 V, AGM Lead Acid batteries
  Data on DC 105-12 provided by FullRiver. Effect of temperature on capacity and lifetime not considered by HOMER
- Solar PV panel - Fixed with no tracking, Oriented at south (0^{o}), Slope = 59^{o}
- Wind Turbine - GUS1B and AIR-X

The all system Scenarios that were run using HOMER are presented in Table 2.

Table 2: System Simulation Scenarios

Envir. Data	Hybrid							Wind only	Solar only (Suntech)
	GUS 1B						Air-X		
	Suntech				Sanyo		Suntevh		
	35W	57W	35W Temp. Effect	Dimming 57W	35W	57W	35W	35W	35W
CEI	Scenario: 3 (6.4)	Scenario: 1 (6.1)	Scenario: 3.1 (6.8)	Scenario: 10 (6.3)	Scenario: 4 (6.5)	Scenario: 2 (6.2)	Scenario: 31 (6.11)	Scenario: 7 (6.6)	Scenario: 8 (6.7)
TIA	Scenario: 5 (6.9)				Scenario: 6 (6.10)		Scenario: 32 (6.12)		

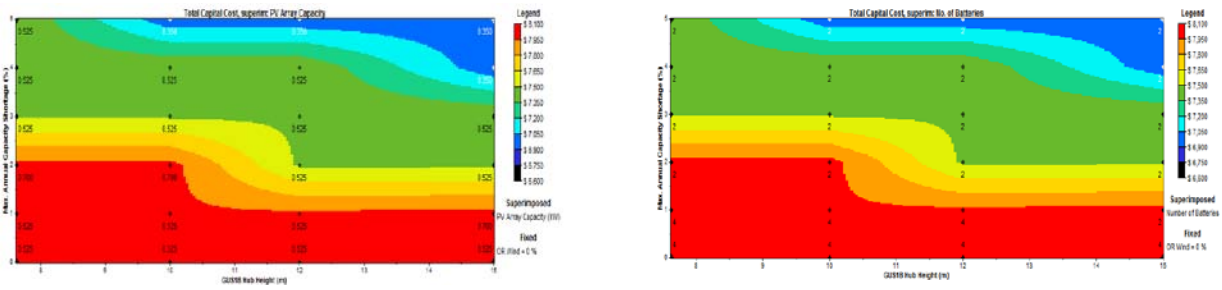

Figure 9: Surface plot results of Scenarios

6.1 Scenario No.1 - CEI Data, Gus1B, 175W Suntech, Fullriver 105Ah, 57 W

Scenarios were run with a sensitivity analysis on wind turbine hub height vs capacity shortage, with storage capacity and solar inputs as variables. The system uses the Suntech 175W solar module. The results are shown in Figure 9.

6.2 Results and Discussion

For the wind turbine hub height 7.62 m and 0 % capacity shortage the optimal system is consisted of 3 PV Panels, one Wind Turbine and 4 Batteries. From the surface plot (Figure 9) it can be seen that hub height changes have no noticeable impact on system configuration. As the system capacity shortage increases the number of PV panels and number of batteries is decreased or remains the same due to the price difference of components. For higher hub heights the capacity shortage is lowered due to greater wind power output. The monthly average electric power output for the system capacity shortage 0% and 5%, 35W load and different wind turbine's hub heights is shown in Figure 10. As can be seen from Figure 10 at all hub heights more power is generated in case of 5 % capacity shortage since the number of PV panels is higher. The monthly average electric power output for the system capacity shortage 0 % and 5 %, 57 W load and different wind turbine's hub heights is presented in Figure 11.

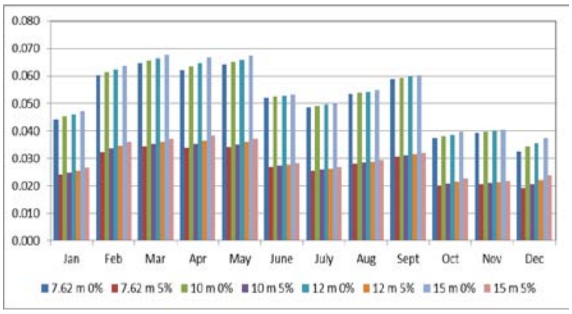

Figure 10: Monthly Average Electric Productions (kW). Load: 35W

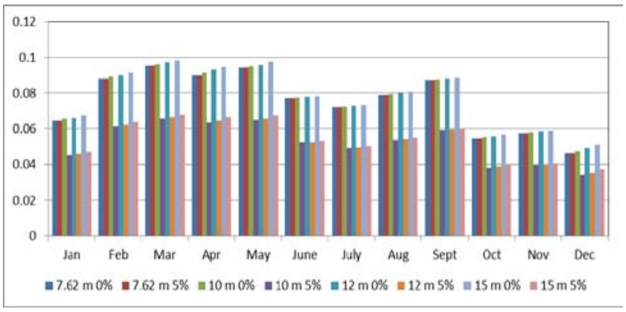

Figure 11: Monthly Average Electric Productions (kW). Load: 57W

The wind turbine's monthly average electric production for the system capacity shortage 0% and 5%, 35 W load and different wind turbine's hub heights is presented in Figure 12. Monthly average power output (kW) from wind turbine is shown in Figure 12.

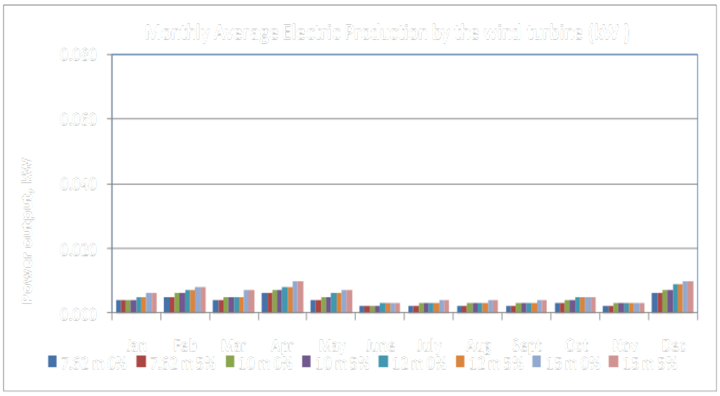

Figure 12: Wind Turbine's Monthly Average Power Output (kW)

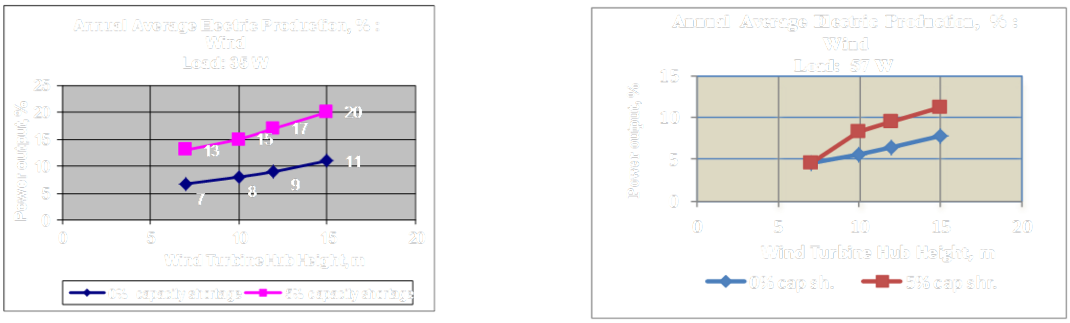

Figure 13: Wind Turbine's Annual Average Power Output (%): (a) Load 35W and (b) Load 57W

As can be seen from Figure 12 the wind turbine's power output varies from month to month, and it is higher in winter-spring period. The maximum values of wind turbine's electric production are for the months – December, January, February and April. The Wind turbine's annual average power output (%) for 35 W and 57 W loads is shown in Figure 13.

The Figure 13(a) shows that the contribution of wind power is 7% at 7.62 m hub height and 11% at 15m hub height in case of 0 % maximum annual capacity shortage. On the other hand, the contribution of wind power is 13% at 7.62 m hub height and 20% at 15 m hub height for 5 % capacity shortage [Figure 13(a)]. The Figure 13(b) shows that the contribution of wind power is 5% at 7.62 m hub height and 8% at 15 m hub height in case of 0 % maximum annual capacity shortage. On the other hand, the contribution of wind power is 5% at 7.62 m hub height and 11% at 15 m hub height for 5 % capacity shortage [Figure 13(b)]. The monthly average electric power output for the system capacity shortage 0% and 5%, 35W load and different wind turbine's hub heights is presented in Figure 14. It shows that not only for 0 % capacity shortage but also for 5 % capacity shortage at all hub heights most of the power (approximately 90 %) is generated by PV panels.

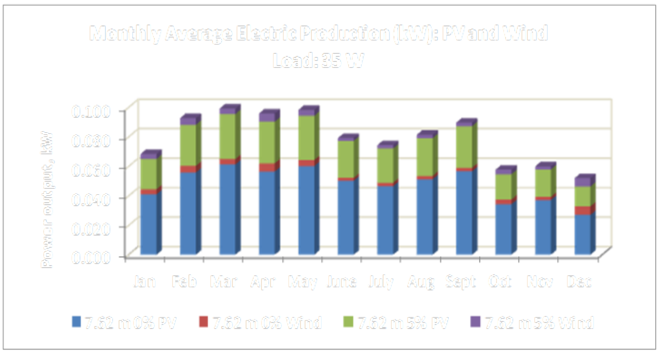

Figure 14: Monthly Average Electric Productions (kW) at hub height: (a) 7.62 m.

7. Conclusions

The analysis of the simulated scenarios results leads to the following conclusions:

- In summary, the 10-min solar/wind resolution data has an impact on the hybrid solar/wind system design. The CEI data was real time data which was incorporated in HOMER for simulation whereas the TIA data was monthly average data for over a 30 year period which was converted into high resolution data by HOMER using pre-determined models.
- The differences are not impressive (dramatic), however, leading to the conclusion that when relevant high resolution meteorological data are not available, publically available monthly averaged (monthly resolution) environmental data (Environment Canada, NASA, etc.) can be used effectively in a tested analysis software like HOMER.
- The annual averaged battery state of charge for the system with Sanyo PV panels was 90% and for the one with Suntech PV panels was 88% though Sanyo generated 518 kWh and Suntech generated 420 kWh of electrical energy. For having zero hours of unmet load Sanyo PV module is better to be used than Suntech PV panel; however, the price of the Sanyo PV panel is 50% higher than that of the Suntech PV panel.
- The analysis of the individual contributions towards annual energy output of solar and wind components of the systems for hybrid-powered street lights of 7.62 m height, situated in the Greater Toronto Area, revealed that the GUS 1B Vertical Axis Wind Turbine contributes only 7% for the least energy storage system using Suntech PV panels and 6% for the least energy storage system using Sanyo PV panels.
- The hybrid system (2 PV, 1 Wind Turbine, 2 Batteries) with AIR-X wind turbine was having 8 hours more unmet load than the system with GUS-1B though AIR-X wind turbine has a higher rated capacity of 0.4 kW. The cut-in speed was 4 m/s for AIR-X turbine and 3 m/s for GUS-1B wind turbine.
- In the period of November to January, when the wind speeds are typically higher (stronger) than for other months, the contribution of from the wind turbine varies from 6% to 17%. For the remainder of the year the wind turbine is inefficient. To have a significant effect under the conditions analyzed, a wind turbine with lower (1.5-2.5 m/s) cut-in speed is required.

References

Borowy, B.S., Salameh, Z.M., Methodology for optimally sizing the combination of a battery bank and PV array in a wind/PV hybrid system. *IEEE Transactions on Energy Conversion* 11 (2), 367–373, 1996.

Climate Weather Office, Available: http://climate.weatheroffice.gc.ca/prods_servs/normals_ documentatione. html#wmo.

Diaf S., Diaf D., Belhamel M., Haddadi M. and Louche A., A methodology for optimal sizing of autonomous hybrid PV/wind system. *Energy Policy*, Vol.35, Issue 11, pp. 5708-5718, 2007.

Eftichios Koutroulis, Dionissia Kolokotsa, Antonis Potirakis and Kostas Kalaitzakis, Methodology for Optimal Sizing of Stand-Alone Photovoltaic/Wind-Generator Systems Using Genetic Algorithms, *Solar Energy*, Vol. 80, 9, pp. 1072 – 1088, 2006.

Ekren Banu Y., Ekren O., Simulation based size optimization of a PV/wind hybrid energy conversion system with battery storage under various load and auxiliary energy conditions. *Applied Energy*, Vol. 86, Issue 9, pp. 1387-1394, 2009.

Ekren Orhan, Ekren Banu Y., Size optimization of a PV/wind hybrid energy conversion system with battery storage using response surface methodology. *Applied Energy*, Vol. 85, Issue 11, pp. 1086-1101, 2008.

Environnement Canada: Available: http://www.ec.gc.ca/meteo-weather/default.asp?lang=En&n=FDF98F96-1 (since 1871).

Kellogg, W.D. et al., Generation unit sizing and cost analysis for stand-alone wind, photovoltaic and hybrid wind/PV systems. *IEEE Transactions on Energy Conversion* 13 (1), 70–75, 1998.

Lambert, T., Gilman, P., Lilienthal, P., Micropower system modeling with HOMER. In Integration of alternative sources of energy, Farret, F.A. and Simões, M.G., John Wiley & Sons, pp. 379-418, 2006.

National Renewable Energy Laboratory (NREL): HOMER Getting Started Guide, Version 2.0. Golden, Colorado, May 2003. Available at http://www.nrel.gov/homer, accessed October 26, 2005.

RETScreen International Renewable Energy Decision Support Centre: *Chapter 2: Wind Energy Project Analysis*. Minister of Natural Resources Canada, 2001-2002. Available at http://www.retscreen.net, accessed October 26, 2005.

Taskin S., Dursun B., Alboyaci B., Performance assessment of a combined solar and wind system. The Arabian *Journal for Science and Engineering*, Vol. 34, Number 1B, pp. 217 – 227, 2009.

Thevenard D, Driesse A, Pelland S, Turcotte D, Poissant Y. Uncertainty in long-term photovoltaic yield predictions, report # 2010-122 (RP-TEC), CanmetENERGY, Varennes Research Center, *Natural Resources Canada*, 52 pp, March 31 2010.

Tina, G., Gagliano, S., Raiti, S., Hybrid solar/wind power system probabilistic modeling for long-term performance assessment. *Solar Energy* 80, 578–588, 2006.

Yang Hongxing, Zhou Wei, Lu Lin, Fang Zhaohong, Optimal sizing method for stand-alone hybrid solar–wind system with LPSP technology by using genetic algorithm. *Solar Energy* 82, pp. 354–367, 2008.

Yang, H.X., Burnett, L., Lu, L., Weather data and probability analysis of hybrid photovoltaic–wind power generation systems in Hong Kong. *Renewable Energy* 28, 1813–1824, 2003.

Yang, H.X., Lu, L., Zhou, W., A novel optimization sizing model for hybrid solar–wind power generation system. *Solar Energy* 81, 1, 76–84, 2007.